## Title

Systems toxicogenomics of prenatal low-dose BPA exposure on liver metabolic pathways, gut microbiota, and metabolic health in mice



## Authors

Diamante, Graciel
Cely, Ingrid
Zamora, Zacary
et al.

## Publication Date

2021

## DOI

10.1016/j.envint.2020.106260

Peer reviewed

HHS Public Access

Author manuscript

*Environ Int*. Author manuscript; available in PMC 2021 January 02.

Published in final edited form as:

*Environ Int*. ; 146: 106260. doi:10.1016/j.envint.2020.106260.

# Systems toxicogenomics of prenatal low-dose BPA exposure on liver metabolic pathways, gut microbiota, and metabolic health in mice

**Graciel Diamante**[a,b], **Ingrid Cely**[a], **Zacary Zamora**[a], **Jessica Ding**[a,c], **Montgomery Blencowe**[a,c], **Jennifer Lang**[d], **Abigail Bline**[b], **Maya Singh**[a], **Aldons J. Lusis**[d,e], **Xia Yang**[a,b,f,*]

[a]Department of Integrative Biology and Physiology, University of California, Los Angeles (UCLA), Los Angeles, CA 90095, USA

[b]Molecular Toxicology Interdepartmental Program, University of California, Los Angeles (UCLA), Los Angeles, CA 90095, USA

[c]Interdepartmental Program of Molecular, Cellular and Integrative Physiology, University of California, Los Angeles (UCLA), Los Angeles, CA 90095, USA

[d]Department of Medicine/Division of Cardiology, University of California, Los Angeles, CA (UCLA), Los Angeles, CA 90095, USA

[e]Department of Microbiology, Immunology and Molecular Genetics, University of California, Los Angeles (UCLA), Los Angeles, CA 90095, USA

[f]Institute for Quantitative and Computational Biosciences, University of California, Los Angeles (UCLA), Los Angeles, CA 90095, USA

## Abstract

Bisphenol A (BPA) is an industrial plasticizer widely found in consumer products, and exposure to BPA during early development has been associated with the prevalence of various cardiometabolic diseases including obesity, metabolic syndrome, type 2 diabetes, and cardiovascular diseases. To elucidate the molecular perturbations underlying the connection of low-dose prenatal BPA exposure to cardiometabolic diseases, we conducted a multi-dimensional systems biology study assessing the liver transcriptome, gut microbial community, and diverse metabolic phenotypes in both male and female mouse offspring exposed to 5 μg/kg/day BPA during gestation. Prenatal



*Corresponding author at: Department of Integrative Biology and Physiology, University of California, Los Angeles, Los Angeles, CA 90095, USA. xyang123@ucla.edu (X. Yang).

CRediT authorship contribution statement

**Graciel Diamante:** Conceptualization, Investigation, Methodology, Formal analysis, Visualization, Writing - original draft, Writing - review & editing. **Ingrid Cely:** Methodology, Investigation, Visualization, Writing - original draft, Writing - review & editing. **Zacary Zamora:** Writing - original draft, Writing - review & editing. **Jessica Ding:** Formal analysis. **Montgomery Blencowe:** Formal analysis, Visualization. **Jennifer Lang:** Investigation. **Abigail Bline:** Methodology. **Maya Singh:** Visualization. **Aldons J. Lusis:** Resources. **Xia Yang:** Supervision, Conceptualization, Writing - review & editing.

Declaration of Competing Interest

The authors declare that they have no known competing financial interests or personal relationships that could have appeared to influence the work reported in this paper.

Appendix A. Supplementary material

Supplementary data to this article can be found online at https://doi.org/10.1016/j.envint.2020.106260.

exposure to low-dose BPA not only significantly affected liver genes involved in oxidative phosphorylation, PPAR signaling and fatty acid metabolism, but also affected the gut microbial composition in an age- and sex-dependent manner. Bacteria such as those belonging to the *S24–7* and *Lachnospiraceae* families were correlated with offspring phenotypes, differentially expressed liver metabolic genes such as *Acadl* and *Dgat1*, and key drivers identified in our gene network modeling such as *Malat1* and *Apoa2*. This multiomics study provides insight into the relationship between gut bacteria and host liver genes that could contribute to cardiometabolic disease risks upon low-dose BPA exposure.

**Keywords**

Bisphenol A; Gut microbiota; Liver transcriptome; Metabolic syndrome; Endocrine disruptor; Systems toxicogenomics

## 1. Introduction

The prevalence of cardiometabolic disorders, such as obesity, metabolic syndrome, type 2 diabetes (T2D), and cardiovascular diseases (CVD) has been increasing at a high rate. For instance, a study evaluating the prevalence of diabetes in the US showed that around 40% of the participants were classified as diabetic or pre-diabetic (Cowie et al., 2009). There has also been an alarming increase in the prevalence of obesity and metabolic syndrome in both adults and children (Dehghan et al., 2005; Smith, 2007; Sahoo et al., 2015). Among the risk factors for cardiometabolic disorders is exposure to environmental contaminants such as endocrine disrupting compounds (EDCs) (National Academies of Sciences, 2018). EDCs are a heterogenous group of chemicals that include pesticides, pharmaceutical agents, and industrial chemicals present in all compartments of the environment (Diamanti-Kandarakis et al., 2009). Among environmental EDCs, bisphenol A (BPA) is one of the most extensively studied due to its broad, global exposure. Humans are consistently exposed to BPA as a result of its ability to leach from consumer goods in plastic and lined metal containers (Sun et al., 2006; Tsai, 2006; Vandenberg et al., 2007; Calafat et al., 2008). According to several studies, the adult human BPA intake can range from 30 ng to 1 μg/kg/day (Kang et al., 2006; Lakind and Naiman, 2008, 2011; Huang et al., 2017; Huang et al., 2018). Currently, the no observed adverse effect level (NOAEL) is 5 mg/kg/day and tolerable daily intake level (TDI) in the U.S. is 50 μg/kg/day according to the EPA (EPA, 2010; Almeida et al., 2018). Moreover, animal studies using exposure doses below TDI (e.g. 0.5 μg-10 μg/kg/day) have shown significant effects on various health endpoints (Richter et al., 2007; Marmugi et al., 2012; Ziv-Gal et al., 2015; Lejonklou et al., 2017).

BPA exposure has been linked to increased body weight, obesity, insulin resistance, diabetes, and cardiovascular diseases in both human epidemiological and animal studies, although not without controversy (Teppala et al., 2012; Beydoun et al., 2014; Ranciere et al., 2015; Han and Hong, 2016; Hao et al., 2017; Mouneimne et al., 2017; Rubin et al., 2017; Wassenaar et al., 2017; Le Magueresse-Battistoni et al., 2018). The controversies in BPA findings are likely due to its complex effects. First, BPA effects are non-monotonic and vary significantly by exposure window (developmental vs adulthood) and dosages. In terms of

exposure window, previous studies have suggested that the *in utero* period is a critical time point for BPA vulnerability (Liu et al., 2013). BPA has the capacity to cross the placenta and has been observed in both maternal and fetal plasma (Takahashi and Oishi, 2000; Schonfelder et al., 2002; Nishikawa et al., 2010). However, the effects and mechanisms of prenatal exposure remain poorly understood, particularly at low doses mimicking human exposure. Second, males and females have been reported to exhibit different BPA responses; however, sex-specific differences have yet to be fully elucidated. Lastly, previous molecular studies of BPA exposure have implicated the involvement of numerous tissues and molecular pathways. In particular, the liver and gut microbiome communities, which are important for metabolic health, have been found to play a role in BPA-induced adverse effects (Malaise et al., 2017; Meng et al., 2019; Shu et al., 2019; Feng et al., 2020). The establishment of the microbiome during childhood is not only important for normal development, but also plays a critical role in health status later in life (Ihekweazu and Versalovic, 2018). The microbial community is critical in maintaining homeostasis of the gut-liver axis, and the liver also plays a role in shaping the intestinal microbial communities (Tripathi et al., 2018; Albillos et al., 2020). Modulation of the intricate relationship between the host and microbiome can contribute to the development of many diseases such as cancer, metabolic, cardiovascular, immune and neurobehavioral disorders (Wallace et al., 2011; Sanz et al., 2015; Mayer and Hsiao, 2017; Tang et al., 2017; Vuong et al., 2017; Vivarelli et al., 2019). The role of gut microbiome-liver interactions has not been investigated for prenatal exposure to BPA at a human relevant dose.

To address the remaining gaps in our understanding of BPA activities as outlined above, we conducted a multi-dimensional systems biology study to examine the influence of prenatal low-dose BPA exposure on offspring across a broad range of metabolic parameters, liver transcriptome, and the gut microbiome in both sexes. We chose to use 5 μg/kg/day since it is a dose below TDI but has been shown to cause developmental effects. In addition, when considering the human to mouse dose conversion factor, this dosage is close to the range of estimated daily human intake (Nair and Jacob, 2016). Compared to most previous studies that have examined different molecular aspects separately, our study design allows for systematic investigation of the multidimensional connections across biological domains such as identifying bacteria that are associated with liver genes, pathways and metabolic phenotypes. Our study provides valuable insight into how BPA, particularly at a low dose, disrupts the gut microbiome-liver axis and elucidates the sex-specific molecular mechanisms involved that contribute to metabolic disorders.

## 2. Materials and methods

### 2.1. Chemicals

Due to the poor solubility of BPA, we first dissolved 1 g of BPA (Milipore Sigma, Cat. No.239658–50G, USA) into 3 mL of pure ethyl alcohol (Sigma-Aldrich, Cat. No. E7023, USA). This mixture was then added to 97 mL of corn oil (Fisher Scientific, Cat. No S25271, USA) to make a stock solution at 10 μg/μL concentration of BPA and 3% ethanol. The stock solution was further diluted as follows: 5 mL of the stock was added to 95 mL of corn oil to make Dilution One at a BPA concentration of 0.5 μg/μL and 0.15% of ethanol. Then, 2.5 mL

of Dilution One was added to 247.5 mL of corn oil to make Dilution Two (working solution), which was at a BPA concentration of 0.005 μg/μL and 0.0015% ethanol. The appropriate amount of Dilution Two was added into a 1/2 Honey Nut Cheerio (treat) (Honey Nut Cheerio, General Mills) to have a final exposure dose of 5 μg/kg/day of BPA. The control group also received a treat with corn oil and the same amount of ethanol (0.0015%) as the BPA-treated group. Both control and treatment groups were administered with the appropriate amount of BPA and corn oil in the treat, according to body weight, for 19–21 consecutive days.

### 2.2. Animal care and BPA exposure

Eight-week-old female and male C57BL/6J mice were purchased from JAX Laboratory (Bar Harbor, ME, USA). Eight breeding pairs, each consisting of one female and one male mouse, were housed in BPA-free opaque cages with glass bottle water dispensers. Mice were maintained on a 12-hour light/dark cycle environment and were given *ad libitum* access to food and water. Food and water intake were measured throughout the breeding period. Mice were fed “Select Rodent Diet 50 IF/6F 5V5R” chow (Newco Distributors, Inc, Rancho Cucamonga, CA, USA) consisting of 50 ppm total isoflavones (genistein, daidzein and glycitein) to regulate dietary estrogenic activity. Due to low survival rate of litters from first-time breeders, the first litter of each breeding pair was removed from the experiment. Male breeders were removed at the time of litter birth to ensure that new pregnancies did not occur until after a repository period. Female mice did not receive any treatment during the first-time breeding phase of the experiment. A week after giving birth to the first litter, females were paired up with the corresponding males from the first breeding round. One or two days after breeding pairs were set up, a vaginal sperm plug was observed to confirm mating. After mating was confirmed, treatment of 5 μg/kg/day BPA or corn oil was administered to female mice for 19–21 consecutive days during the gestation period. Male mice did not receive any BPA or corn oil administration at any point during the experiment. BPA or corn oil treatment was administered every evening between 8 pm and 10 pm. BPA or corn oil was loaded into the treat with a pipette with caution to ensure no loss or leaking of the chemical or control solution. During the treatment period, female breeders were removed from their home cage and weighed in order to prepare the proper dosage of BPA or corn oil daily. Mice were individually placed into empty BPA-free opaque cages with only the treat containing BPA or corn oil and returned to home cages after full consumption. Treatment consumption time took up to two hours for the first few days until acclimation to the new environment was established. Within a few days, female mice consumed the treat within 10 min and were quickly returned to their home cage. BPA and corn oil treatments were terminated after 19–21 days (gestation period) in preparation for pup delivery. After delivery of pups, male breeders were removed from breeding cages. Pups were checked for milk spots regularly to ensure that dams were nursing. At three weeks of age, pups were weaned from each breeding cage and separated into new BPA-free opaque cages with glass bottle water dispensers according to sex with 3–4 mice per cage. Randomization of pups from different breeding cages was done by distributing pups from the same breeding cage into different cages to reduce the risk of cage effects. Each breeding pair had litter sizes ranging from 3 to 8 pups. Litter size was normalized by distributing small (3–5 pups) and large (6–8) litter sizes equally into new cages. Pup cages were maintained on a 12-hour light/dark cycle

environment and were given *ad libitum* access to food and water. Metabolic phenotypes such as body weight was monitored weekly starting at two weeks of age until 24 weeks by weighing mice on a scale. Plasma levels of lipids and glucose tolerance were also measured, as detailed below. Fecal samples were taken at 11, 14, and 20 weeks of age and liver samples were collected at 24 weeks of age, as described below. At the end of the experiment, liver and white adipose tissues were collected and weighed. Liver tissues were subject to lipid assays, as detailed below. All experimental procedures were approved by the UCLA Animal Research Committee.

### 2.3. Intraperitoneal glucose tolerance test (IPGTT)

Male and female offspring mice were tested for disturbances in glucose metabolism using IPGTT at 10 and 21 weeks of age. Mice were fasted overnight for 14 hours prior to testing and had access to drinking water at all times. A 20% glucose solution was prepared for the IP injection (2 g of glucose/ kg body mass). A small incision was made on the mouse tail using a sterile scalpel blade to obtain a blood sample for the glucometer (<5 μL). Baseline glucose for mice was obtained prior to 20% glucose IP injection. Blood glucose was measured at 15, 30, 60 and 120 min post glucose injection to test clearance of glucose.

### 2.4. Plasma lipid and insulin quantification

To investigate possible perturbations in lipid and glucose metabolism in mice exposed to BPA *in utero*, plasma lipid, and insulin quantifications were performed following blood collection by retro-orbital bleeding. Briefly, mice were fasted overnight for 14 hours prior to being anesthetized with isoflurane for blood collection via retro-orbital bleeding using a microcapillary tube at seven weeks of age. Approximately 1% of total body weight of blood was collected into K2 EDTA tubes and placed on ice. To obtain plasma, blood was spun at 1500 g for 10 min at 4 °C and then stored at −80 °C. Plasma triglyceride (pTG), total cholesterol (pTC), high-density lipoprotein (pHDL), unesterified cholesterol (pUC), free fatty acid (pFFA), and insulin (pInsulin) were analyzed using enzymatic colorimetric assays at UCLA GTM Mouse Transfer Core as previously described (Meng et al., 2016). Plasma very low-density lipoprotein (pVLDL) was calculated using the formula: VLDL= (TG/5) and low-density lipoprotein (pLDL) was calculated using the formula: LDL = TC - HDL – VLDL.

### 2.5. Liver lipid assays

Lipids were extracted from liver samples using the Folch method as previously described (Folch et al., 1957). Briefly, approximately 60 mg of liver tissue was homogenized in methanol then incubated overnight in a 2:1 mixture of chloroform and methanol. After filtration, magnesium chloride was added to the mixture and centrifuged. The resulting aqueous phase and soluble proteins were aspirated. The remaining phase was evaporated using nitrogen gas then the dried lipids were dissolved in 1% Triton X-100 in chloroform. The samples were again dried and then resuspended in 1.8% Triton X-100 in water. Samples were then stored in −80 °C prior to lipid analysis. Liver triglyceride (livTG), total cholesterol (livTC), unesterified cholesterol (livUC), phospholipids (livPC) levels were measured using a colorimetric assay at the UCLA GTM Mouse Transfer Core.

### 2.6. Fecal collection

Fecal samples were collected at weeks 11, 14, and 20 from male and female offspring mice. At the time of fecal collection, mice were removed from their home cages and individually placed in an empty autoclaved BPA-free opaque cage without bedding or access to food or water. Mice were allowed to defecate undisturbed. The time of fecal collection was at the beginning of the 12-hour dark cycle. Using sterilized tweezers, 3–5 pieces of fecal samples were collected into sterile 2 mL Eppendorf tubes and flash frozen in liquid nitrogen. Tweezers were thoroughly cleaned in between sample collections with 80% ethanol. Samples were then stored at −80 °C until analysis.

### 2.7. 16S rRNA sequencing and data analysis

DNA was isolated from fecal samples using the PowerSoil DNA Isolation Kit (Mo Bio, Carlsbad, CA) and the bacterial 16S rRNA gene was amplified for amplicons spanning the variable region 4 (V4) using barcoded primers. The amplicons from different samples were pooled, purified, and sequenced using the Illumina HiSeq4000 instrument. Microbial sequence data was analyzed using QIIME 2 (version 2018.6). Sequencing reads were denoised and clustered into amplicon sequence variants using DADA2 (Callahan et al., 2016). Using DADA2, the reads were truncated at 150 bases to obtain only sequences with quality control measure above 33. Resulting sequences were taxonomically classified against Greengenes reference sequences (McDonald et al., 2012). To compare the control and BPA groups, principal coordinates analysis (PCoA) was performed using the Bray-Curtis dissimilarity indices, and principal component analysis (PCA) was performed using Hellinger-transformed amplicon sequence variant (ASV) abundances. For each ASV, DESeq2 was used to compare the abundances between BPA and control groups at each time point within each sex to obtain p values for differential abundance between groups. The p-values were adjusted using the Benjamini-Hochberg (BH) method to estimate false discovery rate (FDR). ASVs that resulted in an FDR < 0.05 were considered significant. The ASVs altered by BPA exposure were then compared across time points and sexes to identify consistent microbes affected by BPA.

### 2.8. Liver RNA sequencing (RNAseq) and data analysis

The whole liver tissue was dissected out upon terminal sacrifice at 24 weeks of age. A portion of the right lobe was then collected, flash frozen in liquid nitrogen, and stored in −80 °C until RNAseq analysis. RNA was extracted from the liver tissues using the MiRNeasy Mini Kit purchased from Qiagen following the manufacturer's instruction (Hilden, Germany). Liver samples used were from mice randomly selected from litters of different dams from independent cages (n = 4/group/sex). The RNA concentration and quality of all 16 liver samples were measured using the Thermo Scientific NanoDrop instrument (Waltham, MA) and the Agilent High Sensitivity RNA ScreenTape System (Agilent, Santa Clara, CA). Libraries were prepared using the Total RNA Library Prep Kit with Ribo-Zero Gold (Illumina, San Diego, CA). Single-end read sequencing was performed on an Illumina Hiseq4000 system. After sequencing, the read quality was assessed using FastQC (http://www.bioinformatics.babraham.ac.uk/projects/fastqc). After quality control, sequence alignment and transcript assembly were done using the HISAT-StringTie pipeline (Pertea et

al., 2016). Reads were mapped to the GRCm38/mm10 reference genome (https://genome.ucsc.edu/index.html). Identification of differentially expressed genes (DEGs) were conducted using DEseq2 (Love et al., 2014) and FDR was estimated using the BH method. Genes with an FDR < 0.01 were considered significant. To investigate the pathways enriched in the BPA-associated DEGs, we used Gene Set Enrichment Analysis (GSEA) (Mootha et al., 2003; Subramanian et al., 2005) to annotate the DEGs with known biological pathways curated from the Kyoto Encyclopedia of Genes and Genomes (KEGG) (Kanehisa and Goto, 2000). KEGG pathways at FDR < 0.05 were considered significant. Fisher's exact test was applied to evaluate the significance of overlapping genes and pathways between DEG sets, such as between male and female liver DEGs. The RNAseq data has been submitted to the Gene Expression Omnibus (GEO) under accession number GSE155845.

### 2.9. Identification of transcription factor (TF) and non-TF regulators using network analyses

To perform network analyses on the liver DEGs identified, we used Mergeomics (https://bioconductor.org/packages/devel/bioc/html/Mergeomics.html) to identify key regulators (Shu et al., 2016). To identify potential TFs important for the BPA-induced effects, we first assessed whether BPA-associated DEGs were downstream targets of specific liver TFs using Marker Set Enrichment Analysis (MSEA). Liver tissue TF regulatory networks were obtained from the FANTOM5 database (Marbach et al., 2016). Using MSEA, we evaluated the enrichment of BPA-induced DEGs within the target genes for each TF. We then used Weighted Key Driver Analysis (wKDA) to identify potential non-TF network regulators using previously constructed liver Bayesian networks (Zhu et al., 2007; Zhu et al., 2008; Shu et al., 2019). In brief, these networks were built using multiple large mouse and human liver transcriptome and genetic datasets. To identify key drivers (KDs), we searched for nodes/genes whose neighboring subnetworks were enriched for BPA-induced DEGs in the liver. TFs or non-TF network regulators with FDR < 5% were considered statistically significant. The cytoscape software was used for network visualization (Shannon et al., 2003).

### 2.10. Correlation analysis between gut microbiota and metabolic phenotypes or liver signature genes

To investigate the relationships among the liver transcriptome, gut microbiome, and metabolic phenotypes affected by low-dose BPA exposure, correlation analysis was performed. We first correlated the abundance of significantly altered microbial ASVs with metabolic phenotypes, including body weight, area under the curve (AUC) for glucose tolerance, plasma insulin, plasma lipids, liver lipids and tissue weight (liver and adipose). The bacteria significantly correlated with phenotypes were then correlated to liver DEGs affected by BPA. Correlation was assessed using Biweight midcorrelation (bicor), which is robust to outliers. P-values were adjusted using the BH approach and FDR < 0.05 was considered significant. The BPA-affected genes demonstrating significant bacterial correlations were evaluated for enriched KEGG pathways using the GSEA tool. Pathways and biological functions at FDR < 0.05 were considered significant.

# 3. Results

## 3.1. Low-dose BPA exposure in utero exhibits sex-specific effects on metabolic phenotypes in offspring

After *in utero* BPA exposure, various metabolic phenotypes of the offspring were monitored. In female offspring, significantly increased body weight in BPA-treated mice was observed at 13, 14, 20 and 22 weeks of age compared to controls (Fig. 1A). IPGTT results used to evaluate glucose tolerance was not altered in females at both week 10 and week 21 timepoints (Fig. 1B–1D). There was also no effect observed for plasma insulin (pInsulin) levels (Fig. 1E). In contrast, BPA-treated male offspring showed a significant decrease in body weight at week 4 (Fig. 1F) and faster glucose clearance based on the IPGTT results at week 10 and 21 week (Fig. 1G–1I) in the absence of significant changes in fasting plasma insulin levels (Fig. 1J). These results suggest enhanced insulin sensitivity in BPA-treated males. We also measured circulating plasma lipids in female and male offspring (pTG, pFFA, pTC, pUC, pHDL, pLDL and pVLDL). BPA-treated female mice did not show significant changes in any of the plasma lipid traits (Fig. 1K) compared to control mice. BPA-treated male mice showed significantly decreased pTG, pFFA, pUC, and pVLDL, but not pTC, pHDL, or pLDL (Fig. 1L). Lipids in the liver (livTG, livTC, livUC, livPC) were also measured. In BPA-treated females, there was a significant decrease in livTG levels (Fig. 1M). However, in males there was an increase in livTC and livUC (Fig. 1N). In both females and males, no difference was observed in the liver and adipose weight (Fig. 1O–1P). There was a significant difference in tissue weight to body weight ratio for liver but not for adipose in BPA-treated females (Fig. 1Q). No effect in tissue weight to body weight ratio in males was observed (Fig. 1R). Overall, our findings suggest sex-specific differences in BPA-induced metabolic phenotypes.

## 3.2. Low-dose BPA exposure in utero affects liver transcriptome and pathways in both male and female offspring

To investigate the host tissue responses to low-dose BPA exposure, RNAseq was performed on offspring liver tissue. As a result, 1958 DEGs (1001 down-regulated and 957 up-regulated) were observed in the females and 1429 DEGs (788 down-regulated and 641 up-regulated) were observed in the males (FDR < 0.01) (Fig. 2A and B; full DEG list in Supplementary Table 1). There were 817 common DEGs between males and females (454 down-regulated and 363 up-regulated), which represents a significant overlap in DEGs between sexes (fold enrichment = 7.026, $p < 1.0e{-}100$ by Fisher's exact test) (Fig. 2C–E) despite the differences in the phenotypic manifestations and certain unique gene expression changes in each sex.

Pathway enrichment analysis of all DEGs in female showed 99 overrepresented KEGG pathways (Fig. 2F; full pathway list in Supplementary Table 2) and male all DEGs were enriched for 89 KEGG pathways (Fig. 2G; full pathway list in Supplementary Table 2). When comparing the pathways between sexes, 73 were common (fold enrichment = 1.541, $p = 1.1e{-}15$) (Fig. 2H), including oxidative phosphorylation, neurodegenerative diseases, PPAR signaling, fatty acid metabolism, and insulin signaling. Female-specific pathways

included thyroid cancer and gluconeogenesis, while T cell receptor, regulation of autophagy and mTOR signaling were unique for males (Fig. 2H).

When considering only the down-regulated DEGs, 30 pathways were overlapping between females (41 pathways) and males (54 pathways) (fold enrichment = 2.520, p = 1.3e-12), including oxidative phosphorylation, neurodegenerative diseases, and WNT signaling. Pathways such as thyroid cancer and cardiac muscle disease were unique for the females while xenobiotic metabolism and T and B cell receptor signaling were unique for the males among the downregulated DEGs (Fig. 2I; full pathway list in Supplementary Table 2).

When only considering the up-regulated DEGs, 26 pathways were common between females (61 pathways) and males (33 pathways) (fold enrichment = 2.402; p = 1.8e−10), including oxidative phosphorylation, neurodegenerative diseases and glutathione metabolism. Drug metabolism and ABC transporter are examples of pathways that were unique for the females while ECM receptor interaction and fatty acid metabolism were unique for the males among the up-regulated DEGs (Fig. 2J; full pathway list in Supplementary Table 2).

The above results indicate that numerous metabolic pathways were perturbed in both males and females in addition to certain sex-specific pathways, which could underlie the observed sex-specific differences in phenotypic manifestation.

### 3.3. Identification of TF and non-TF regulators potentially governing BPA induced molecular perturbations

To explore the TFs that likely regulate the liver DEGs affected by BPA exposure, we leveraged liver-specific TF regulatory networks from the FANTOM5 project and identified TFs whose target genes were enriched in BPA DEGs. At FDR < 5%, there were 13 and 18 TFs identified in males and females, respectively (Full TF list in Supplementary Table 3). There were six (e.g. *Tfeb, Nr5a1, Egr4*) unique TFs identified in males and 11 TFs (e.g. *Rora, Srebf2, Hnf4*) in females (Fig. 3A and B). The male-specific TFs identified play roles in lysosomal biogenesis, development, and mitogenesis. Female-specific TFs play roles in cholesterol homeostasis, lipid metabolism, and liver development. There were also seven TFs (*Zfp143*, *Yy1*, *Elf5*, *Etv5*, *Elk4*, *Etv1* and *Arnt*) shared between sexes (Fig. 3C). The common TFs are involved in drug metabolism, cell growth and differentiation, and circadian rhythm.

To identify regulatory genes that mediate the action of BPA on downstream targets through non-TF mechanisms, we leveraged data-driven liver-specific Bayesian networks (BNs) to predict gene-gene regulatory relationships and identify key drivers (KDs) of the BPA DEGs. At FDR < 0.05, we identified 35 and 36 KDs in male and female offspring, respectively (Full KD list in Supplementary Table 4). The top five unique KDs identified in males were *Capza2, Apoa2, Ttr, Sepp1 and Akr1c12* (Fig. 3D). The top male KDs have roles in lipid metabolism, protein transport, and hormone metabolism. In females, the top five unique KDs were *Ktn1, Tmed5, Golga4, F2 and Sult1a1* (Fig. 3E). The female KDs are involved in hemostasis, xenobiotic clearance, and protein transport. There were four shared KDs identified between male and female offspring (*Dcxr, Erbb2ip, Tlk1* and *Malat1*) (Fig. 3F). The common KDs have functions in lipid pathways, xenobiotic metabolism, and chromatin

assembly. These KDs, along with the identified TFs from the above analysis, may represent the regulatory targets which transmit the *in vivo* biological effects of BPA.

### 3.4. Low-dose prenatal BPA exposure affects the abundance and diversity of gut microbial species in both male and female offspring

Next, to investigate the effects of low-dose BPA exposure on the gut microbiota, 16S rRNA sequencing was performed on feces collected from both male and female offspring at 11, 14, and 20 weeks of age. Diversity metrics were used to evaluate community composition within a sample. As shown in the rarefaction curves based on observed ASVs, the number of ASVs detected increased and plateaued as the number of extracted sequences increased, verifying the sequencing depth was appropriate to observe all sample species (Fig. 4A). Alpha diversity was calculated using the Shannon diversity index, which indicated no significant difference between treatments (Fig. 4B). Next, differences in the gut communities between BPA- treated animals and controls were evaluated. Both PCoA based on Bray-Curtis distance and PCA using Hellinger-transformed abundance of the gut microbial community showed that the BPA groups clustered separately from the control offspring (Fig. 4C and D) in an age-dependent manner, with the most pronounced effect observed at week 20. We observed fluctuations in the abundance of bacterial families such as *Bifidobacteriaceae*, *Bacteriodaceae* and *S24–7* at different stages (Fig. 4E).

We then analyzed the abundance of specific ASVs between BPA-treated and control samples. In females, we identified 55, 63, and 71 differentially abundant ASVs in week 11, 14 and 20, respectively (Fig. 5A; full ASV list in Supplementary Table 5). Among these, seven ASVs (*Oscillospira*, *Prevotella*, YS2, members of the *Rikenellaceae*, *Lachnospiraceae*, and *Ruminococcaceae* families with unknown species, and member of the order Clostridiales unknown species) were consistently significant in females at all time points (Fig. 5A–C). *Prevotella* was found in all time points in control samples while its abundance was low or not observed in BPA-treated samples in the female offspring (Fig. 5B). In the male offspring, we identified 112, 137, and 108 differentially abundant ASVs in week 11, 14, and 20, respectively (Fig. 5D; full ASV list in Supplementary Table 6), among which 30 ASVs (e.g. *Lactobacillus*, *Coprococcus*, *Dehalobacterium*, *Ruminococcus*, and *Streptococcus*) were consistently significant at all time points (Fig. 5D). *Lactobacillus* had decreased abundance in the BPA-treated samples at all time points in males (Fig. 5E). Interestingly, among the ASVs consistently altered in all time points between female and male offspring there were four ASVs in common, one of which belongs to the *Rikenellaceae* family (Fig. 5C and F). This ASV was increased in the BPA-treated mice regardless of sex.

### 3.5. Relationship among host metabolic phenotypes, gut microbiota, and liver genes in response to low-dose BPA

To evaluate the relationship between the gut microbiota, host liver genes, and metabolic phenotypes, we first correlated microbial ASVs that showed alterations by BPA at any given time point with metabolic phenotypes collected from the same sets of mice. There was a total of 21 and three different ASVs correlated to metabolic phenotypes in female and male offspring, respectively (Fig. 5G; full correlation list in Supplementary Table 7). In females, many of the ASVs correlating with phenotypes belonged to the S24–7 (Fig. 5H), and several

belonged to the *Erysipelotrichaceae* and *Lachnospiraceae* families. Of the 21 ASVs correlated to female phenotypes, two (YS2 and *Prevotella*) were consistently altered across all three time points. The remaining were only significant in one (nine ASVs) or two time points (ten ASVs). Out of the 21 phenotype-correlated ASVs, 18 were significantly correlated to body weight and 5 were correlated to pTG and pVLDL levels. There were two ASVs (*Lactobacillus* and S24–7 unknown species) that were correlated to body weight, pTG and pVLDL. In the male offspring, none of the three correlated ASVs were consistently altered across time points; each ASV was unique to a specific time point. There were no significantly correlated bacteria to insulin or any of the lipids quantified in either plasma or liver in males. Only one ASV was correlated to body weight. This bacterium was identified as part of the *Allobaculum* genus which belongs to the *Erysipelotrichaceae* family. The other two ASVs were correlated to glucose tolerance AUC. One bacterium belonged to the *S24–7* family (Fig. 5I) and the other to the order Clostridiales.

Next, we examined the correlation between the phenotype-correlated ASVs and liver DEGs. Among the 21 ASVs correlated with female phenotypes, only seven ASVs were correlated to BPA-responsive liver DEGs (Table 1; full correlation list in Supplementary Table 8). Among these seven ASVs, four belong to the Clostridiales order and two belonged to the *S24–7* family, and the DEGs correlated to bacterial abundance were enriched for pathways such as oxidative phosphorylation, RNA metabolism, glycan biosynthesis and insulin signaling (Table 1; full pathway list in Supplementary Table 9). Among these correlated DEGs, several were KDs, such as *F2*, *Malat1* and *Ktn1* (Table 1). For the three male ASVs correlating with body weight or glucose tolerance, two ASVs (Clostridiales and *S24–7* both unknown species) showed correlations with liver DEGs involved in oxidative phosphorylation, drug metabolism, mTOR signaling and fatty acid metabolism (Table 1; full correlation list in Supplementary Table 8; full pathway list in Supplementary Table 10;). Among these correlated DEGs, several were also KDs in our network analysis, such as *Apoa2, Akr1c12* and *Malat1* (Table 1). These results suggest connections between the liver-gut axis and metabolic phenotypes.

## 4. Discussion

Previous studies that examined developmental exposure to BPA at higher concentrations have reported effects on liver and gut microbiome separately. In our current study, we uniquely looked at the effect of low-dose BPA exposure (5 μg/kg/day) on the gut-liver axis from the same animals in both male and female offspring exposed *in utero*. This systematic multiomics investigation (tens of metabolic phenotypes, gut microbiome, and liver transcriptome) allowed us to investigate the relationship across molecular and phenotypic domains. Our study is the first to show that in samples obtained from the same animals, abundances of certain bacteria are correlated with liver gene expression and diverse metabolic phenotypes, supporting a relationship between the gut microbiome, the host liver, and metabolic perturbations induced by low-dose, prenatal BPA exposure (Fig. 6). Importantly, we found sex-specific differences in metabolic phenotypes, liver transcriptome, and gut bacteria, although consistencies were found primarily in various metabolic pathways such as oxidative phosphorylation and PPAR signaling. Different BPA-altered bacteria in male and female offspring were also correlated with liver DEGs which are involved in

different aspects of metabolism. In this study, the specific microbial species and the associated pathways in host liver tissues revealed insights into the molecular mechanisms through which BPA exposure contributes to metabolic risk, opening unique opportunities to modulate gut bacteria to neutralize EDC adverse effects.

In the present study, we observed differences between the male and female offspring in BPA-induced metabolic phenotypes (Fig. 6). Agreeing with the distinct metabolic phenotypes between sexes, our study of the liver transcriptome also revealed unique pathways perturbed by low-dose prenatal BPA exposure between male and female offspring that potentially play a role in determining phenotypic differences (Fig. 6). Specifically, *in utero* BPA-exposed females had a significant increase in body weight in adulthood compared to the BPA-exposed males. This increase in body weight in females occurred despite no alteration in white adipose tissue weight, suggesting that other tissues not evaluated are potentially affected by BPA. The female DEGs were uniquely enriched for glycan biosynthesis pathway, which has been shown to be important in shaping the gut microbiota and is important for metabolic health (Koropatkin et al., 2012). Agreeing with this, the glycan pathway was also correlated to BPA affected bacteria such as *S24–7*, which has been linked to diverse metabolic phenotypes including body weight. Therefore, the glycan pathway may underlie the weight phenotype seen in females. In contrast to females, males had a significant decrease in weight at an early timepoint. This was accompanied with lower plasma lipid levels such as TG, which is consistent with our previous prenatal study at 5 mg/kg/day of BPA (Shu et al., 2019). However, this is in contrast to other studies that have reported an increase in plasma TG (Lejonklou et al., 2017). When evaluating all the liver DEGs a pathway identified for males was mTOR signaling which has been linked to restricted fetal growth (Hart et al., 2019). Our study at both the phenotypic and liver transcriptome levels in general confirms significant sex-specific differences in metabolic related processes such as energy metabolism noted in BPA studies and reviews (Mackay et al., 2013; Strakovsky et al., 2015; Nadal et al., 2017; Marraudino et al., 2018), but uniquely point to sex-specific pathways such as glycan biosynthesis for females and mTOR for males. In addition, our study found that xenobiotic metabolism pathways were enriched in downregulated DEGs in males but were enriched in upregulated DEGs in females, which could also contribute to the sex-specific phenotypes observed. Enzymes involved in xenobiotic metabolism have been shown to play a role in metabolic diseases (Xu et al., 2016). Altered expression of important enzymes in xenobiotic metabolism such as the cytochrome p450 family have been observed in different diabetic and obesity mouse models and can affect disease susceptibility (Roe et al., 1999; Yoshinari et al., 2006; Kudo et al., 2009; Kumar et al., 2018; Heintz et al., 2019). Along with the sex-specific pathways, our study showed shared liver pathways between male and female offspring such as oxidative phosphorylation, PPAR signaling pathways, and fatty acid metabolism (Fig. 6). Despite these shared pathways, we did not identify consistencies between sexes at the phenotypic level. As liver is not the only tissue involved in metabolism, it is possible that interactions of these liver pathways with sex-specific pathways in other tissues not examined here contribute to unique metabolic phenotypes between sexes.

To put our results from low-dose prenatal exposure in the broader context of previous findings and to explore molecular insights into the non-monotomic effects of BPA, we

compared the male liver gene expression changes from our low-dose prenatal exposure study with previous liver transcriptomic studies of different doses and exposure windows. We previously examined the liver transcriptome of male offspring exposed to a high-dose of BPA (5 mg/kg/day) *in utero* (Shu et al., 2019). There were 114 genes in common between the two prenatal studies of different dosages (Supplementary Fig. 1). Pathways such as drug metabolism, PPAR signaling, and fatty acid metabolism were some of the common pathways identified between studies. Pathways related to oxidative phosphorylation and VEGF signaling were unique for the current low-dose study, while steroid hormone biosynthesis and glycolysis/gluconeogenesis were unique for the high-dose study. We also compared the male DEGs in the present study to a previous adult BPA exposure study done at 50 μg/kg/day dose in male mice (Marmugi et al., 2012). When comparing all the DEGs regardless of the direction, there were several genes shared between the two studies such as *Sc5d*, *Acacb*, *Slc22a5* and *Erbb2ip*. Moreover, two DEGs (*Slc22a5* and *Sc5d*) were shared across all three studies across dosages and exposure windows. *Slc22a5* plays a role in carnitine transport, which is important for fatty acid metabolism (Longo et al., 2016). *Sc5d* is gene that encodes for an enzyme involved in cholesterol synthesis (Krakowiak et al., 2003). These pathways and genes consistently affected by BPA exposure at different dosages and exposure windows point to the core processes underlying the cardiometabolic effects of BPA exposure. Overall, the phenotypic and molecular alterations induced by BPA are complex and are driven by differences in experimental design, dose and sex.

To provide insights into potential regulators of liver transcriptomic and pathway alterations, we took several complementary approaches. We first used different network modeling approaches, including TF networks and Bayesian gene regulatory networks, to predict key regulators. The TF-based analysis revealed unique TFs in male (e.g. *Tfeb* and *Egr4*) and female (e.g. *Srebf2* and *Rora*) offspring as well as shared TFs (e. g. *Arnt* and *Zfp143*). The BN approach also identified unique KDs in male (e.g. *Apoa2* and *Ttr*) and females (e.g. *Sult1a1* and *F2)* as well as common KDs (e.g. *Malat1* and *Dcxr*) (Fig. 6). These network regulators could mediate the BPA effects on downstream genes and pathways in the liver. We then examined the gut microbiome composition of the offspring at multiple ages. We found certain bacteria to be consistently altered at all time points, whereas, others were only altered at one time point measured (Fig. 6). This shows the dynamic nature of the gut microbiome and the importance of evaluating microbial changes at multiple time points. BPA-exposed offspring had marked changes in the relative abundances of different groups within the Firmicutes phylum, the order Clostridiales, and families *Lachnospiraceae*, *Ruminococcaceae*, *Erysipelotrichaceae*, and *Lactobaciliaceae*. Previous BPA studies done on various doses have also revealed a change in the relative abundance of bacteria in the Firmicutes families, such as *Ruminococcaceae*, and *Lachnospiraceae*, which produce short-chain fatty acids (SCFAs) (Lai et al., 2016; Xu et al., 2019). A shift in bacterial composition from Bacteroidetes to Firmicutes has been previously identified as a marker for cardiometabolic risk (Rosenfeld, 2017). A fall in Bifidobacteria and certain Clostridia groups have also been observed in response to both perinatal and direct BPA exposure and decreases in these bacteria are linked to obesity and diabetes (Larsen et al., 2010; Lai et al., 2016; Malaise et al., 2017). In our current study, we also observed a decrease in the *Bifidobacteriaceae* and *Clostridiaceae* families at the early time points (weeks 11 and 14) but

an increase at the latest time point (week 20). Given that the rise of these families occurred at the latest time point, it may be of interest to examine how their dynamic fluctuations play a role in occurrence of metabolic phenotypes in future studies.

By evaluating multiomics data together from the same animals after *in utero* low-dose BPA exposure, our study allows direct integration and assessment of the relationships between the multidimensional data, a significant departure from previous studies that investigate each aspect separately. In our study, we identified specific bacterial classes that are significantly influenced by prenatal low-dose BPA exposure and correlated with metabolic phenotypes (Fig. 6). In females, we identified several bacteria belonging to the clostridia class and *S24–7* family to be correlated to body weight. In contrast, in males, the bacterial abundance of a member of the *S24–7* was correlated with glucose tolerance. These correlated bacteria are important for maintenance of gut homeostasis. Interestingly, abundances of bacteria from the *S24–7* family have been reported to be altered in obese models, during liver regeneration, disease remission, and in a myriad of other gut-microbiome responses (Liu et al., 2016; Ormerod et al., 2016; Lagkouvardos et al., 2019). Additionally, the *S24–7* family have also been implicated in providing oxidative stress protection (Ormerod et al., 2016). Due to the challenges in characterizing and culturing the *S24–7* family, it is difficult to directly test their role in cardiometabolic disease pathogenesis.

Our data also uniquely identified several BPA-responsive bacteria to be correlated to liver DEGs. Pathway enrichment analysis of the DEGs correlated to the BPA-responsive bacteria were enriched for core metabolic pathways such as oxidative phosphorylation, PPAR signaling pathways and fatty acid metabolism (Fig. 6). These results support potential interactions between gut microbiome and liver upon BPA exposure. Several of the important metabolic DEGs were correlated to specific bacteria. In females, the abundance of *Coprococcus* was correlated to the expression of *Acadl* and KD *Malat1*. *Coprococcus* belongs to the family *Lachnospiraceae* and is involved in the production of SCFAs (Louis et al., 2004; Reichardt et al., 2014; Koh et al., 2016). *Acadl* is a gene that encodes for a member of the acyl-CoA dehydrogenase family, which are enzymes that play a role in energy metabolism (Kurtz et al., 1998). *Malat1* is a long noncoding RNA that regulates genes involved in cancer progression and diabetes (Zhang et al., 2017). In males, the abundance of a member of the *S24–7* family was correlated to two KDs *Acadm* and *Apoa2* (Fig. 6). *Acadm* is a gene that encodes an enzyme that metabolizes fatty acids for energy production. Loss of function in the enzyme produced by *Acadm* results in hypoglycemia (Grosse et al., 2006; Lim et al., 2018). *Apoa2* is gene that encodes for an abundant HDL protein and has a regulatory role in lipid metabolism and atherosclerosis development (Warden et al., 1993). The exact role these bacteria play in regulating the host liver genes and KDs induced by BPA needs to be further studied.

The data presented here in our multiomics study represents the discovery phase of a comprehensive investigation of *in vivo* BPA activities, which opens new opportunities for future testing of the specific findings. However, we acknowledge the following limitations. First, we did not conduct qPCR validation of the RNAseq-based findings. Although using low-throughput qPCRs to validate RNAseq data was a common practice during the early years of RNAseq studies, over the past decades sufficient evidence has been raised to

support the accuracy of RNAseq measurements. In a systematic technical comparison study, the agreement between RNAseq and qRT-PCR was found to be >80% (SEQC/MAQC-III Consortium, 2014), which is consistent with our own findings in several previous studies (Chen et al., 2016; Meng et al., 2016; Meng et al., 2017; Shu et al., 2019). In addition, many DEGs that were significant in our data have also been observed in previous work which provides additional validation to the consistency across completely independent studies. Moreover, our study mainly focuses on identifying the pathways and networks perturbed by BPA instead of the accuracy of individual DEGs. Additional limitations to our study include PCR biases that exist in 16S sequencing, food and water intake measurements were not evaluated which can be affected by BPA exposure (Angle et al., 2013; Laursen et al., 2017; Nadal et al., 2017), and no BPA residue was measured. We also acknowledge that our study mainly identifies correlated molecular factors, and the causality of the altered microbiome and liver genes require future functional studies.

## 5. Conclusion

In summary, our systematic investigation of low-dose BPA prenatal exposure on a range of metabolic phenotypes, the liver transcriptome, and gut microbiota help further elucidate the gut-liver axis involved in metabolic reprogramming. Our data highlights sex-specific and shared pathways affected by BPA in the liver of male and female mice exposed *in utero*. In the same set of mice, we also evaluated the microbiome at multiple time points and identified several bacteria that potentially play a key role in interacting with liver metabolic pathways to regulate metabolic phenotypes induced by BPA. However, future studies are needed to further evaluate how dysbiosis of the gut microbial community can affect the host genome, causing the reprogramming of gene networks in critical metabolic tissues to promote metabolic disease in offspring. Such information may help guide public health policies and help devise novel preventative and therapeutic avenues that engage gut microbiome modulation to counteract environmentally induced metabolic diseases.

## Supplementary Material

Refer to Web version on PubMed Central for supplementary material.

## Acknowledgements

The authors thank Jonnby LaGuardia for assisting in the animal work and Jennifer Garcia for her assistance in RNA sample preparations.

Funding

XY was supported by the National Institutes of Health (DK104363 and DK117850) and the Southern California Environmental Health Sciences Center (P30ES007048). GD was supported by the National Institute of Environmental Health Sciences (T32ES015457) and the American Diabetes Association Postdoctoral Fellowship (1-19-PDF-007-R). AJL was supported by the National Institutes of Health (HL28481 and DK117850). AB was supported by the National Institute of Environmental Health Sciences of the National Institutes of Health (T32ES015457). The above funders had no role in study design; in the collection, analysis and interpretation of data; in the writing of the report; and in the decision to submit the article for publication.

## References


Albillos A, de Gottardi A, Rescigno M, 2020 The gut-liver axis in liver disease: Pathophysiological basis for therapy. J. Hepatol 72, 558–577. [PubMed: 31622696]

Almeida S, Raposo A, Almeida-González M, Carrascosa C, 2018 Bisphenol a: food exposure and impact on human health. Compr. Rev. Food Sci. Food Saf 17, 1503–1517. [PubMed: 33350146]

Angle BM, Do RP, Ponzi D, Stahlhut RW, Drury BE, Nagel SC, Welshons WV, Besch-Williford CL, Palanza P, Parmigiani S, vom Saal FS, Taylor JA, 2013 Metabolic disruption in male mice due to fetal exposure to low but not high doses of bisphenol A (BPA): evidence for effects on body weight, food intake, adipocytes, leptin, adiponectin, insulin and glucose regulation. Reprod. Toxicol 42, 256–268. [PubMed: 23892310]

Beydoun HA, Khanal S, Zonderman AB, Beydoun MA, 2014 Sex differences in the association of urinary bisphenol-A concentration with selected indices of glucose homeostasis among U.S. adults. Ann. Epidemiol 24, 90–97. [PubMed: 23954568]

Calafat AM, Ye X, Wong LY, Reidy JA, Needham LL, 2008 Exposure of the U.S. population to bisphenol A and 4-tertiary-octylphenol: 2003–2004. Environ. Health Perspect 116, 39–44. [PubMed: 18197297]

Callahan BJ, McMurdie PJ, Rosen MJ, Han AW, Johnson AJ, Holmes SP, 2016 DADA2: High-resolution sample inference from Illumina amplicon data. Nat. Methods 13, 581–583. [PubMed: 27214047]

Chen Y, Shu L, Qiu Z, Lee DY, Settle SJ, Que Hee S, Telesca D, Yang X, Allard P, 2016 Exposure to the BPA-substitute bisphenol S causes unique alterations of germline function. PLoS Genet 12, e1006223. [PubMed: 27472198]

Cowie CC, Rust KF, Ford ES, Eberhardt MS, Byrd-Holt DD, Li C, Williams DE, Gregg EW, Bainbridge KE, Saydah SH, Geiss LS, 2009 Full accounting of diabetes and pre-diabetes in the U.S. population in 1988–1994 and 2005–2006. Diabetes Care 32, 287–294. [PubMed: 19017771]

Dehghan M, Akhtar-Danesh N, Merchant AT, 2005 Childhood obesity, prevalence and prevention. Nutr. J 4, 24. [PubMed: 16138930]

Diamanti-Kandarakis E, Bourguignon JP, Giudice LC, Hauser R, Prins GS, Soto AM, Zoeller RT, Gore AC, 2009 Endocrine-disrupting chemicals: an Endocrine Society scientific statement. Endocr. Rev 30, 293–342. [PubMed: 19502515]

EPA, 2010 U.S. Environmental Protection Agency Bisphenol A Action Plan.

Feng D, Zhang H, Jiang X, Zou J, Li Q, Mai H, Su D, Ling W, Feng X, 2020 Bisphenol A exposure induces gut microbiota dysbiosis and consequent activation of gut-liver axis leading to hepatic steatosis in CD-1 mice. Environ. Pollut 265, 114880. [PubMed: 32540565]

Folch J, Lees M, Sloane Stanley GH, 1957 A simple method for the isolation and purification of total lipides from animal tissues. J. Biol. Chem 226, 497–509. [PubMed: 13428781]

Grosse SD, Khoury MJ, Greene CL, Crider KS, Pollitt RJ, 2006 The epidemiology of medium chain acyl-CoA dehydrogenase deficiency: an update. Genet. Med 8, 205–212. [PubMed: 16617240]

Han C, Hong YC, 2016 Bisphenol A, hypertension, and cardiovascular diseases: epidemiological, laboratory, and clinical trial evidence. Curr. Hypertens. Rep 18, 11. [PubMed: 26781251]

Hao M, Ding L, Xuan L, Wang T, Li M, Zhao Z, Lu J, Xu Y, Chen Y, Wang W, Bi Y, Xu M, Ning G, 2017 Urinary bisphenol A concentration and the risk of central obesity in Chinese adults: A prospective study. J. Diabetes.

Hart B, Morgan E, Alejandro EU, 2019 Nutrient sensor signaling pathways and cellular stress in fetal growth restriction. J. Mol. Endocrinol 62, R155–R165. [PubMed: 30400060]

Heintz MM, Kumar R, Rutledge MM, Baldwin WS, 2019 Cyp2b-null male mice are susceptible to diet-induced obesity and perturbations in lipid homeostasis. J. Nutr. Biochem 70, 125–137. [PubMed: 31202118]

Huang RP, Liu ZH, Yin H, Dang Z, Wu PX, Zhu NW, Lin Z, 2018 Bisphenol A concentrations in human urine, human intakes across six continents, and annual trends of average intakes in adult and child populations worldwide: A thorough literature review. Sci. Total Environ 626, 971–981. [PubMed: 29898562]

Huang RP, Liu ZH, Yuan SF, Yin H, Dang Z, Wu PX, 2017 Worldwide human daily intakes of bisphenol A (BPA) estimated from global urinary concentration data (2000–2016) and its risk analysis. Environ. Pollut 230, 143–152. [PubMed: 28649042]

Ihekweazu FD, Versalovic J, 2018 Development of the Pediatric Gut Microbiome: Impact on Health and Disease. Am. J. Med. Sci 356, 413–423. [PubMed: 30384950]

Kanehisa M, Goto S, 2000 KEGG: kyoto encyclopedia of genes and genomes. Nucleic Acids Res 28, 27–30. [PubMed: 10592173]

Kang JH, Kondo F, Katayama Y, 2006 Human exposure to bisphenol A. Toxicology 226, 79–89. [PubMed: 16860916]

Koh A, De Vadder F, Kovatcheva-Datchary P, Backhed F, 2016 From dietary fiber to host physiology: short-chain fatty acids as key bacterial metabolites. Cell 165, 1332–1345. [PubMed: 27259147]

Koropatkin NM, Cameron EA, Martens EC, 2012 How glycan metabolism shapes the human gut microbiota. Nat. Rev. Microbiol 10, 323–335. [PubMed: 22491358]

Krakowiak PA, Wassif CA, Kratz L, Cozma D, Kovarova M, Harris G, Grinberg A, Yang Y, Hunter AG, Tsokos M, Kelley RI, Porter FD, 2003 Lathosterolosis: an inborn error of human and murine cholesterol synthesis due to lathosterol 5-desaturase deficiency. Hum. Mol. Genet 12, 1631–1641. [PubMed: 12812989]

Kudo T, Shimada T, Toda T, Igeta S, Suzuki W, Ikarashi N, Ochiai W, Ito K, Aburada M, Sugiyama K, 2009 Altered expression of CYP in TSOD mice: a model of type 2 diabetes and obesity. Xenobiotica 39, 889–902. [PubMed: 19925381]

Kumar R, Litoff EJ, Boswell WT, Baldwin WS, 2018 High fat diet induced obesity is mitigated in Cyp3a-null female mice. Chem. Biol. Interact 289, 129–140. [PubMed: 29738703]

Kurtz DM, Rinaldo P, Rhead WJ, Tian L, Millington DS, Vockley J, Hamm DA, Brix AE, Lindsey JR, Pinkert CA, O'Brien WE, Wood PA, 1998 Targeted disruption of mouse long-chain acyl-CoA dehydrogenase gene reveals crucial roles for fatty acid oxidation. Proc. Natl. Acad. Sci. USA 95, 15592–15597. [PubMed: 9861014]

Lagkouvardos I, Lesker TR, Hitch TCA, Galvez EJC, Smit N, Neuhaus K, Wang J, Baines JF, Abt B, Stecher B, Overmann J, Strowig T, Clavel T, 2019 Sequence and cultivation study of Muribaculaceae reveals novel species, host preference, and functional potential of this yet undescribed family. Microbiome 7, 28. [PubMed: 30782206]

Lai KP, Chung YT, Li R, Wan HT, Wong CK, 2016 Bisphenol A alters gut microbiome: Comparative metagenomics analysis. Environ. Pollut 218, 923–930. [PubMed: 27554980]

Lakind JS, Naiman DQ, 2008 Bisphenol A (BPA) daily intakes in the United States: estimates from the 2003–2004 NHANES urinary BPA data. J. Expo. Sci. Environ. Epidemiol 18, 608–615. [PubMed: 18414515]

Lakind JS, Naiman DQ, 2011 Daily intake of bisphenol A and potential sources of exposure: 2005–2006 National Health and Nutrition Examination Survey. J. Expo. Sci. Environ. Epidemiol 21, 272–279. [PubMed: 20237498]

Larsen N, Vogensen FK, van den Berg FW, Nielsen DS, Andreasen AS, Pedersen BK, Al-Soud WA, Sorensen SJ, Hansen LH, Jakobsen M, 2010 Gut microbiota in human adults with type 2 diabetes differs from non-diabetic adults. PLoS ONE 5, e9085. [PubMed: 20140211]

Laursen MF, Dalgaard MD, Bahl MI, 2017 Genomic GC-Content Affects the Accuracy of 16S rRNA Gene Sequencing Based Microbial Profiling due to PCR Bias. Front. Microbiol 8, 1934. [PubMed: 29051756]

Le Magueresse-Battistoni B, Multigner L, Beausoleil C, Rousselle C, 2018 Effects of bisphenol A on metabolism and evidences of a mode of action mediated through endocrine disruption. Mol. Cell. Endocrinol 475, 74–91. [PubMed: 29481862]

Lejonklou MH, Dunder L, Bladin E, Pettersson V, Ronn M, Lind L, Walden TB, Lind PM, 2017 Effects of low-dose developmental bisphenol A exposure on metabolic parameters and gene expression in male and female Fischer 344 rat offspring. Environ. Health Perspect 125, 067018. [PubMed: 28657538]

Lim SC, Tajika M, Shimura M, Carey KT, Stroud DA, Murayama K, Ohtake A, McKenzie M, 2018 Loss of the mitochondrial fatty acid beta-oxidation protein medium-chain acyl-coenzyme A

dehydrogenase disrupts oxidative phosphorylation protein complex stability and function. Sci. Rep 8, 153. [PubMed: 29317722]

Liu HX, Rocha CS, Dandekar S, Wan YJ, 2016 Functional analysis of the relationship between intestinal microbiota and the expression of hepatic genes and pathways during the course of liver regeneration. J. Hepatol 64, 641–650. [PubMed: 26453969]

Liu J, Yu P, Qian W, Li Y, Zhao J, Huan F, Wang J, Xiao H, 2013 Perinatal bisphenol A exposure and adult glucose homeostasis: identifying critical windows of exposure. PLoS ONE 8, e64143. [PubMed: 23675523]

Longo N, Frigeni M, Pasquali M, 2016 Carnitine transport and fatty acid oxidation. Biochim. Biophys. Acta, Mol. Cell. Biol. Lipids 1863, 2422–2435.

Louis P, Duncan SH, McCrae SI, Millar J, Jackson MS, Flint HJ, 2004 Restricted distribution of the butyrate kinase pathway among butyrate-producing bacteria from the human colon. J. Bacteriol 186, 2099–2106. [PubMed: 15028695]

Love MI, Huber W, Anders S, 2014 Moderated estimation of fold change and dispersion for RNA-seq data with DESeq2. Genome Biol 15, 550. [PubMed: 25516281]

Mackay H, Patterson ZR, Khazall R, Patel S, Tsirlin D, Abizaid A, 2013 Organizational effects of perinatal exposure to bisphenol-A and diethylstilbestrol on arcuate nucleus circuitry controlling food intake and energy expenditure in male and female CD-1 mice. Endocrinology 154, 1465–1475. [PubMed: 23493373]

Malaise Y, Menard S, Cartier C, Gaultier E, Lasserre F, Lencina C, Harkat C, Geoffre N, Lakhal L, Castan I, Olier M, Houdeau E, Guzylack-Piriou L, 2017 Gut dysbiosis and impairment of immune system homeostasis in perinatally-exposed mice to Bisphenol A precede obese phenotype development. Sci. Rep 7, 14472. [PubMed: 29101397]

Marbach D, Lamparter D, Quon G, Kellis M, Kutalik Z, Bergmann S, 2016 Tissue-specific regulatory circuits reveal variable modular perturbations across complex diseases. Nat. Methods 13, 366–370. [PubMed: 26950747]

Marmugi A, Ducheix S, Lasserre F, Polizzi A, Paris A, Priymenko N, Bertrand-Michel J, Pineau T, Guillou H, Martin PG, Mselli-Lakhal L, 2012 Low doses of bisphenol A induce gene expression related to lipid synthesis and trigger triglyceride accumulation in adult mouse liver. Hepatology 55, 395–407. [PubMed: 21932408]

Marraudino M, Bonaldo B, Farinetti A, Panzica G, Ponti G, Gotti S, 2018 Metabolism Disrupting Chemicals and Alteration of Neuroendocrine Circuits Controlling Food Intake and Energy Metabolism. Front. Endocrinol. (Lausanne) 9, 766. [PubMed: 30687229]

Mayer EA, Hsiao EY, 2017 The gut and its microbiome as related to central nervous system functioning and psychological well-being: introduction to the special issue of psychosomatic medicine. Psychosom. Med 79, 844–846. [PubMed: 28976454]

McDonald D, Price MN, Goodrich J, Nawrocki EP, DeSantis TZ, Probst A, Andersen GL, Knight R, Hugenholtz P, 2012 An improved Greengenes taxonomy with explicit ranks for ecological and evolutionary analyses of bacteria and archaea. ISME J 6, 610–618. [PubMed: 22134646]

Meng Q, Ying Z, Noble E, Zhao Y, Agrawal R, Mikhail A, Zhuang Y, Tyagi E, Zhang Q, Lee JH, Morselli M, Orozco L, Guo W, Kilts TM, Zhu J, Zhang B, Pellegrini M, Xiao X, Young MF, Gomez-Pinilla F, Yang X, 2016 Systems nutrigenomics reveals brain gene networks linking metabolic and brain disorders. EBioMedicine 7, 157–166. [PubMed: 27322469]

Meng Q, Zhuang Y, Ying Z, Agrawal R, Yang X, Gomez-Pinilla F, 2017 Traumatic brain injury induces genome-wide transcriptomic, methylomic, and network perturbations in brain and blood predicting neurological disorders. EBioMedicine 16, 184–194. [PubMed: 28174132]

Meng Z, Tian S, Yan J, Jia M, Yan S, Li R, Zhang R, Zhu W, Zhou Z, 2019 Effects of perinatal exposure to BPA, BPF and BPAF on liver function in male mouse offspring involving in oxidative damage and metabolic disorder. Environ. Pollut 247, 935–943. [PubMed: 30823348]

Mootha VK, Lindgren CM, Eriksson KF, Subramanian A, Sihag S, Lehar J, Puigserver P, Carlsson E, Ridderstrale M, Laurila E, Houstis N, Daly MJ, Patterson N, Mesirov JP, Golub TR, Tamayo P, Spiegelman B, Lander ES, Hirschhorn JN, Altshuler D, Groop LC, 2003 PGC-1alpha-responsive genes involved in oxidative phosphorylation are coordinately downregulated in human diabetes. Nat. Genet 34, 267–273. [PubMed: 12808457]

Mouneimne Y, Nasrallah M, Khoueiry-Zgheib N, Nasreddine L, Nakhoul N, Ismail H, Abiad M, Koleilat L, Tamim H, 2017 Bisphenol A urinary level, its correlates, and association with cardiometabolic risks in Lebanese urban adults. Environ. Monit. Assess. 189, 517. [PubMed: 28942470]

Nadal A, Quesada I, Tuduri E, Nogueiras R, Alonso-Magdalena P, 2017 Endocrine-disrupting chemicals and the regulation of energy balance. Nat. Rev. Endocrinol 13, 536–546. [PubMed: 28524168]

Nair AB, Jacob S, 2016 A simple practice guide for dose conversion between animals and human. J Basic Clin Pharm 7, 27–31. [PubMed: 27057123]

National Academies of Sciences, E., and Medicine., 2018 Environmental Chemicals, the Human Microbiome, and Health Risk: A Research Strategy. The National Academies Press, Washington, DC.

Nishikawa M, Iwano H, Yanagisawa R, Koike N, Inoue H, Yokota H, 2010 Placental transfer of conjugated bisphenol A and subsequent reactivation in the rat fetus. Environ. Health Perspect 118, 1196–1203. [PubMed: 20382578]

Ormerod KL, Wood DL, Lachner N, Gellatly SL, Daly JN, Parsons JD, Dal'Molin CG, Palfreyman RW, Nielsen LK, Cooper MA, Morrison M, Hansbro PM, Hugenholtz P, 2016 Genomic characterization of the uncultured Bacteroidales family S24–7 inhabiting the guts of homeothermic animals. Microbiome 4, 36. [PubMed: 27388460]

Pertea M, Kim D, Pertea GM, Leek JT, Salzberg SL, 2016 Transcript-level expression analysis of RNA-seq experiments with HISAT, StringTie and Ballgown. Nat. Protoc 11, 1650–1667. [PubMed: 27560171]

Ranciere F, Lyons JG, Loh VH, Botton J, Galloway T, Wang T, Shaw JE, Magliano DJ, 2015 Bisphenol A and the risk of cardiometabolic disorders: a systematic review with meta-analysis of the epidemiological evidence. Environ Health 14, 46. [PubMed: 26026606]

Reichardt N, Duncan SH, Young P, Belenguer A, McWilliam Leitch C, Scott KP, Flint HJ, Louis P, 2014 Phylogenetic distribution of three pathways for propionate production within the human gut microbiota. ISME J 8, 1323–1335. [PubMed: 24553467]

Richter CA, Birnbaum LS, Farabollini F, Newbold RR, Rubin BS, Talsness CE, Vandenbergh JG, Walser-Kuntz DR, vom Saal FS, 2007 In vivo effects of bisphenol A in laboratory rodent studies. Reproduct. Toxicol. (Elmsford N.Y.) 24, 199–224.

Roe AL, Howard G, Blouin R, Snawder JE, 1999 Characterization of cytochrome P450 and glutathione S-transferase activity and expression in male and female ob/ob mice. Int. J. Obes. Relat. Metab. Disord 23, 48–53. [PubMed: 10094576]

Rosenfeld CS, 2017 Gut dysbiosis in animals due to environmental chemical exposures. Front. Cell. Infect. Microbiol 7, 396. [PubMed: 28936425]

Rubin BS, Paranjpe M, DaFonte T, Schaeberle C, Soto AM, Obin M, Greenberg AS, 2017 Perinatal BPA exposure alters body weight and composition in a dose specific and sex specific manner: The addition of peripubertal exposure exacerbates adverse effects in female mice. Reprod. Toxicol 68, 130–144. [PubMed: 27496714]

Sahoo K, Sahoo B, Choudhury AK, Sofi NY, Kumar R, Bhadoria AS, 2015 Childhood obesity: causes and consequences. J. Family Med. Prim Care 4, 187–192. [PubMed: 25949965]

Sanz Y, Olivares M, Moya-Perez A, Agostoni C, 2015 Understanding the role of gut microbiome in metabolic disease risk. Pediatr. Res 77, 236–244. [PubMed: 25314581]

Schonfelder G, Wittfoht W, Hopp H, Talsness CE, Paul M, Chahoud I, 2002 Parent bisphenol A accumulation in the human maternal-fetal-placental unit. Environ. Health Perspect 110, A703–A707. [PubMed: 12417499]

SEQC/MAQC-III Consortium, 2014 A comprehensive assessment of RNA-seq accuracy, reproducibility and information content by the Sequencing Quality Control consortium. Nat. Biotechnol 32 (9), 903–914. [PubMed: 25150838]

Shannon P, Markiel A, Ozier O, Baliga NS, Wang JT, Ramage D, Amin N, Schwikowski B, Ideker T, 2003 Cytoscape: a software environment for integrated models of biomolecular interaction networks. Genome Res 13, 2498–2504. [PubMed: 14597658]

Shu L, Meng Q, Diamante G, Tsai B, Chen YW, Mikhail A, Luk H, Ritz B, Allard P, Yang X, 2019 Prenatal bisphenol A exposure in mice induces multitissue multiomics disruptions linking to cardiometabolic disorders. Endocrinology 160, 409–429. [PubMed: 30566610]

Shu L, Zhao Y, Kurt Z, Byars SG, Tukiainen T, Kettunen J, Orozco LD, Pellegrini M, Lusis AJ, Ripatti S, Zhang B, Inouye M, Makinen VP, Yang X, 2016 Mergeomics: multidimensional data integration to identify pathogenic perturbations to biological systems. BMC Genomics 17, 874. [PubMed: 27814671]

Smith SC Jr., 2007 Multiple risk factors for cardiovascular disease and diabetes mellitus. Am. J. Med. 120, S3–S11.

Strakovsky RS, Wang H, Engeseth NJ, Flaws JA, Helferich WG, Pan YX, Lezmi S, 2015 Developmental bisphenol A (BPA) exposure leads to sex-specific modification of hepatic gene expression and epigenome at birth that may exacerbate high-fat diet-induced hepatic steatosis. Toxicol. Appl. Pharmacol 284, 101–112. [PubMed: 25748669]

Subramanian A, Tamayo P, Mootha VK, Mukherjee S, Ebert BL, Gillette MA, Paulovich A, Pomeroy SL, Golub TR, Lander ES, Mesirov JP, 2005 Gene set enrichment analysis: a knowledge-based approach for interpreting genome-wide expression profiles. Proc. Natl. Acad. Sci. USA 102, 15545–15550. [PubMed: 16199517]

Sun C, Leong LP, Barlow PJ, Chan SH, Bloodworth BC, 2006 Single laboratory validation of a method for the determination of Bisphenol A, Bisphenol A diglycidyl ether and its derivatives in canned foods by reversed-phase liquid chromatography. J. Chromatogr. A 1129, 145–148. [PubMed: 16945377]

Takahashi O, Oishi S, 2000 Disposition of orally administered 2,2-Bis(4-hydroxyphenyl)propane (Bisphenol A) in pregnant rats and the placental transfer to fetuses. Environ. Health Perspect 108, 931–935. [PubMed: 11049811]

Tang WH, Kitai T, Hazen SL, 2017 Gut microbiota in cardiovascular health and disease. Circ. Res 120, 1183–1196. [PubMed: 28360349]

Teppala S, Madhavan S, Shankar A, 2012 Bisphenol A and metabolic syndrome: results from NHANES. Int. J. Endocrinol. 2012, 598180. [PubMed: 23251154]

Tripathi A, Debelius J, Brenner DA, Karin M, Loomba R, Schnabl B, Knight R, 2018 The gut-liver axis and the intersection with the microbiome. Nat. Rev. Gastroenterol. Hepatol 15, 397–411. [PubMed: 29748586]

Tsai WT, 2006 Human health risk on environmental exposure to Bisphenol-A: a review. Journal of environmental science and health. Part C, Environ. Carcinogenesis Ecotoxicol. Rev 24, 225–255.

Vandenberg LN, Hauser R, Marcus M, Olea N, Welshons WV, 2007 Human exposure to bisphenol A (BPA). Reprod. Toxicol. 24, 139–177. [PubMed: 17825522]

Vivarelli S, Salemi R, Candido S, Falzone L, Santagati M, Stefani S, Torino F, Banna GL, Tonini G, Libra M, 2019 Gut microbiota and cancer: from pathogenesis to therapy. Cancers (Basel) 11.

Vuong HE, Yano JM, Fung TC, Hsiao EY, 2017 The Microbiome and Host Behavior. Annu. Rev. Neurosci 40, 21–49. [PubMed: 28301775]

Wallace TC, Guarner F, Madsen K, Cabana MD, Gibson G, Hentges E, Sanders ME, 2011 Human gut microbiota and its relationship to health and disease. Nutr. Rev 69, 392–403. [PubMed: 21729093]

Warden CH, Hedrick CC, Qiao JH, Castellani LW, Lusis AJ, 1993 Atherosclerosis in transgenic mice overexpressing apolipoprotein A-II. Science 261, 469–472. [PubMed: 8332912]

Wassenaar PNH, Trasande L, Legler J, 2017 Systematic review and meta-analysis of early-life exposure to bisphenol A and obesity-related outcomes in rodents. Environ. Health Perspect 125, 106001. [PubMed: 28982642]

Xu J, Huang G, Nagy T, Teng Q, Guo TL, 2019 Sex-dependent effects of bisphenol A on type 1 diabetes development in non-obese diabetic (NOD) mice. Arch. Toxicol 93, 997–1008. [PubMed: 30600366]

Xu X, Li R, Chen G, Hoopes SL, Zeldin DC, Wang DW, 2016 The role of cytochrome P450 epoxygenases, soluble epoxide hydrolase, and epoxyeicosatrienoic acids in metabolic diseases. Adv. Nutr 7, 1122–1128. [PubMed: 28140329]

Yoshinari K, Takagi S, Sugatani J, Miwa M, 2006 Changes in the expression of cytochromes P450 and nuclear receptors in the liver of genetically diabetic db/db mice. Biol. Pharm. Bull. 29, 1634–1638. [PubMed: 16880618]

Zhang X, Hamblin MH, Yin KJ, 2017 The long noncoding RNA Malat 1: Its physiological and pathophysiological functions. RNA Biol 14, 1705–1714. [PubMed: 28837398]

Zhu J, Wiener MC, Zhang C, Fridman A, Minch E, Lum PY, Sachs JR, Schadt EE, 2007 Increasing the power to detect causal associations by combining genotypic and expression data in segregating populations. PLoS Comput. Biol 3, e69. [PubMed: 17432931]

Zhu J, Zhang B, Smith EN, Drees B, Brem RB, Kruglyak L, Bumgarner RE, Schadt EE, 2008 Integrating large-scale functional genomic data to dissect the complexity of yeast regulatory networks. Nat. Genet 40, 854–861. [PubMed: 18552845]

Ziv-Gal A, Wang W, Zhou C, Flaws JA, 2015 The effects of in utero bisphenol A exposure on reproductive capacity in several generations of mice. Toxicol. Appl. Pharmacol 284, 354–362. [PubMed: 25771130]

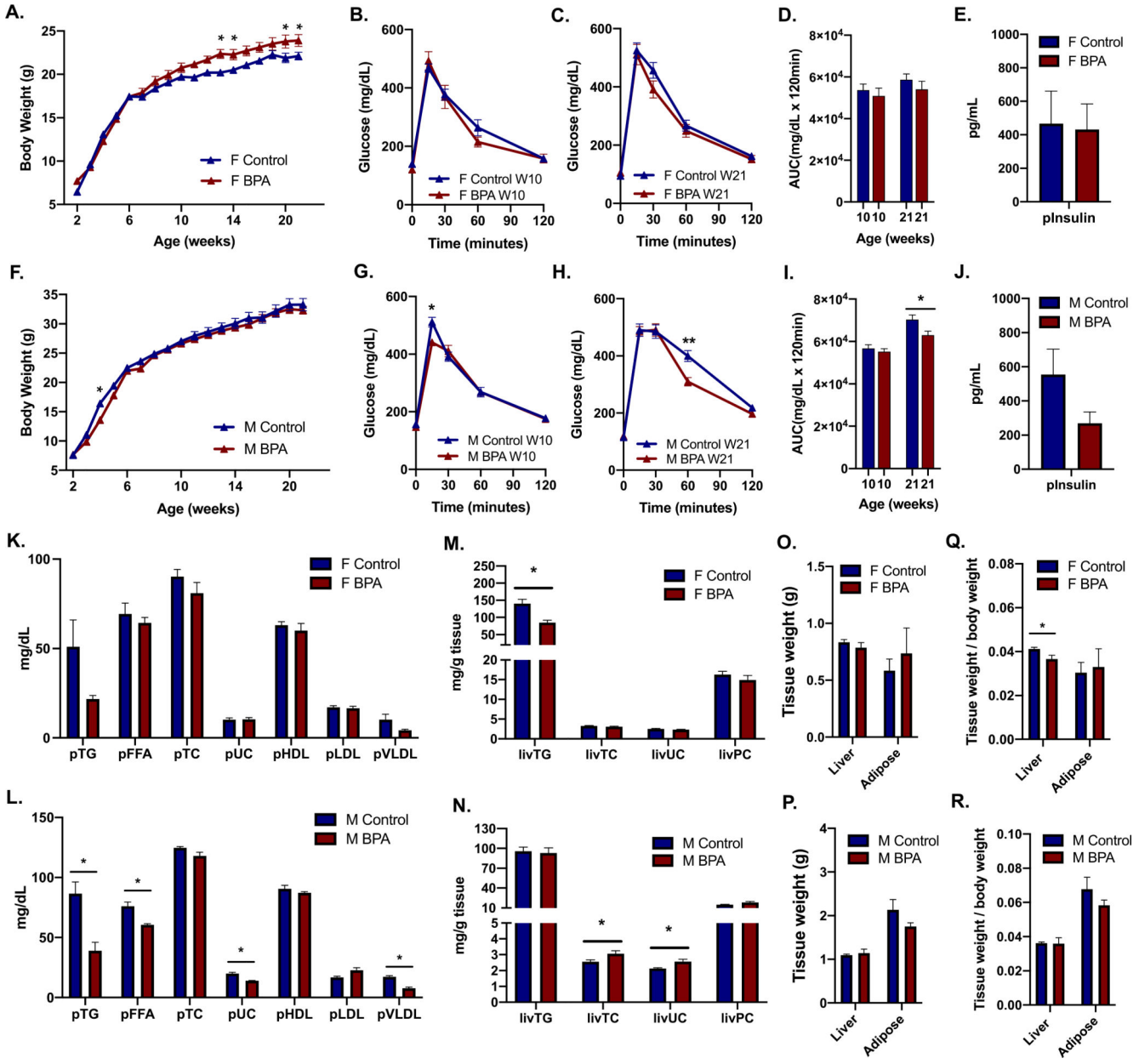


**Fig. 1.**

Metabolic phenotypes of offspring exposed to BPA *in utero*. Female offspring average body weight (A) and glucose tolerance test at 10 weeks (B) and 21 weeks (C) of age after *in utero* BPA exposure. Bar plot of glucose tolerance AUC in female offspring (D). Female fasting insulin (pInsulin) levels in plasma at 7 weeks (E). Male offspring average body weight (F) and glucose tolerance test at 10 weeks (G) and 21 weeks (H) of age after *in utero* BPA exposure. Bar plot of glucose tolerance AUC in male offspring (I). Male fasting insulin (pInsulin) levels in plasma at 7 weeks (J). Bar plot of female (K) and male (L) plasma lipid profiles at 7 weeks. Plasma triglycerides (pTG), free-fatty acids (pFFA), total cholesterol (pTC), unesterified cholesterol (pUC), high-density lipoprotein (pHDL), low-density lipoprotein (pLDL), very low-density lipoprotein (pVLDL). Bar plot of female (M) and male

(N) liver lipid profiles: liver triglycerides (livTG), total cholesterol (livTC), unesterified cholesterol (livUC), phospholipids (livPC). Bar plot of the liver and white adipose weight in females (O) and males (P). Bar plot of the tissue weight to body weight ratio of liver and white adipose in females (Q) and males (R). Data are shown as means ± S.E; n = 6–10 per group/sex. Statistical analysis was performed using 2-way ANOVA followed by Bonferroni's multiple comparisons test (A-C, F-H). Statistical analysis was performed using a two-tailed Student's *t*-test for unpaired comparisons (D, E, I, J, K-R). Asterisk (*) represents p-value ≤ 0.05.

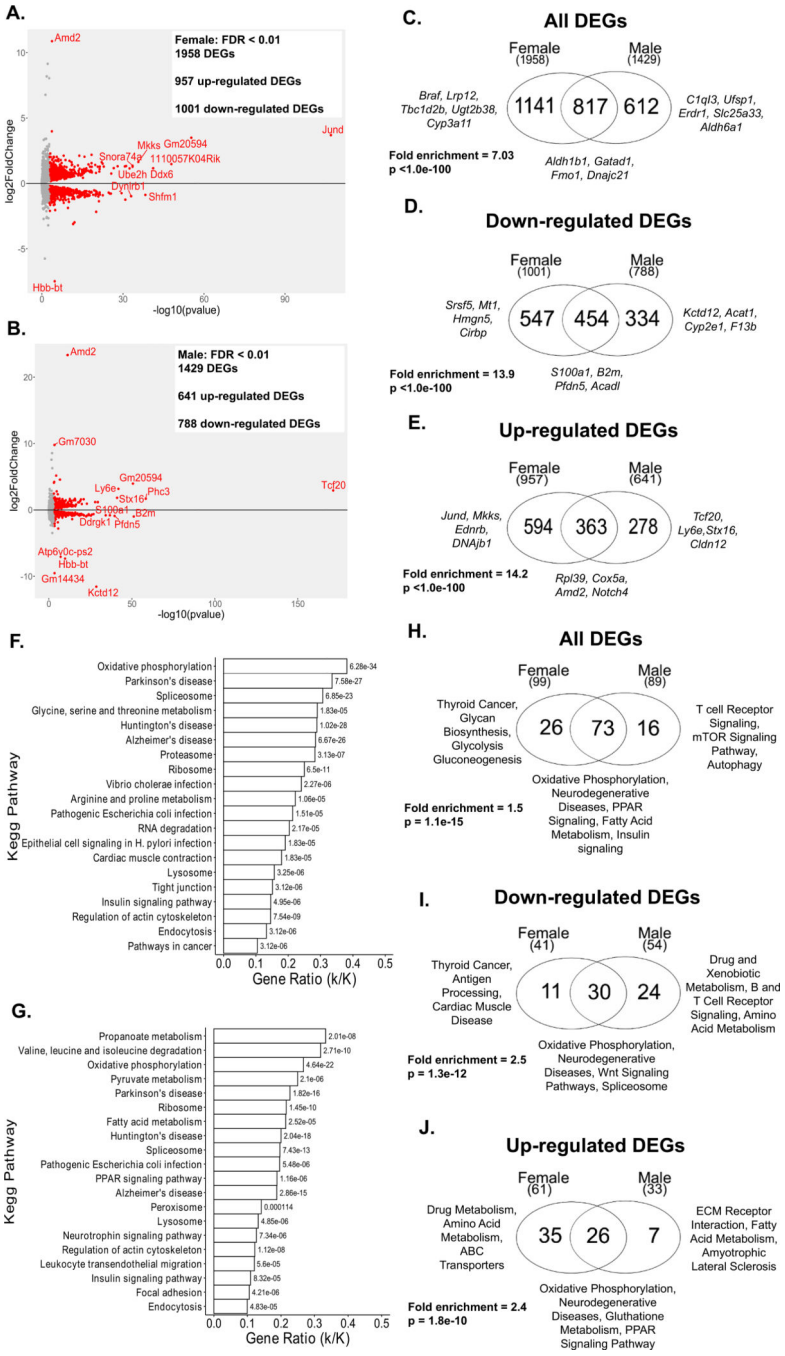


**Fig. 2.**

Liver transcriptomic alterations and pathway enrichment analysis of differentially expressed genes (DEGs) in the liver of male and female offspring exposed to BPA *in utero*. Volcano plots of differentially expressed genes (DEGs) identified in the female (A) and male (B) offspring determined by Deseq2 analysis. Red dots represent significant genes FDR < 0.01. Venn diagram comparing all DEGs (C), down-regulated DEGs (D), and up-regulated DEGs (E) in female and male liver transcriptome analysis. Significant overlap was determined by Fisher's exact test. Bar plot of top 20 enriched Kegg pathways identified in the female (F)

and male (G) offspring. Enrichment FDR q-value (shown beside the bars) was determined by GSEA. Venn diagram comparing the significant Kegg pathways identified using all DEGs (H), down-regulated DEGs (I), and up-regulated DEGs (J) in female and male liver transcriptome analysis. Significant overlap was determined by Fisher's exact test. Sample size n = 4 per group/sex. (For interpretation of the references to colour in this figure legend, the reader is referred to the web version of this article.)

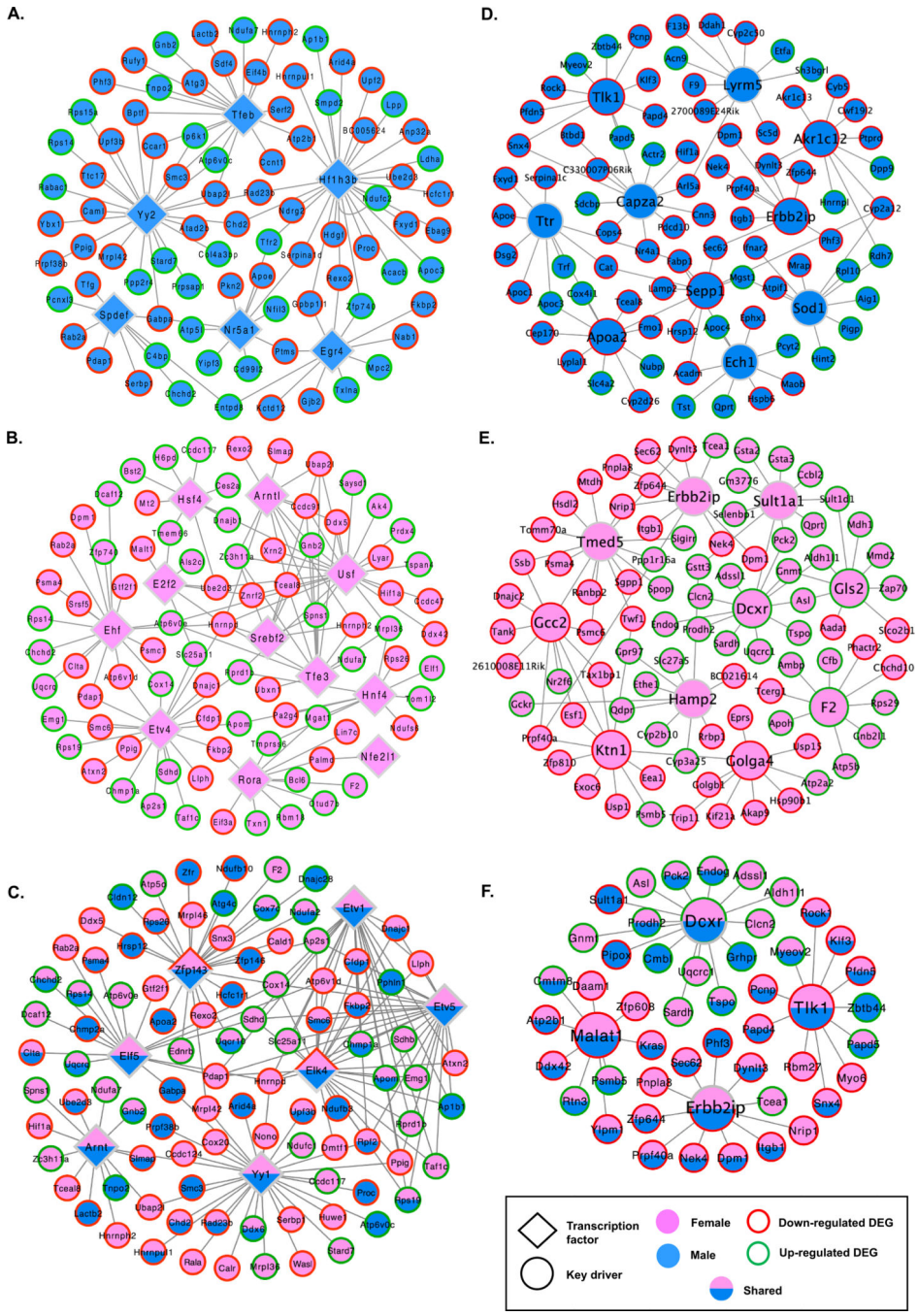


**Fig. 3.**

Transcription factor and key driver analysis of BPA-induced liver gene expression changes. Liver transcription factor (TF) regulatory networks unique to male (A), female (B), and shared among male and female (C). Networks are of significant TFs (FDR < 5%) identified based on enrichment of liver DEGs among TF downstream targets. TFs are represented as diamond-shaped nodes while known DEG targets are represented as circles. Topology of the network was based on FANTOM5. Only network edges that are also DEGs are presented. For the male (A) transcription factor network, DEGs shown are those with a FDR < 1e-3.

For the female (B) and shared transcription factor network, DEGs shown are those with a FDR < 1e-5. Gene-gene regulatory subnetworks of top 10 key drivers (KD) in male (D), female (E) and shared among male and female offspring (F). Networks are of the top 10 KDs (FDR < 5%) identified based on enrichment of liver DEGs. Topology of the network was based on Bayesian modeling of liver datasets from mouse and human. KDs are represented as larger circular nodes. DEGs shown had a FDR < 0.01.

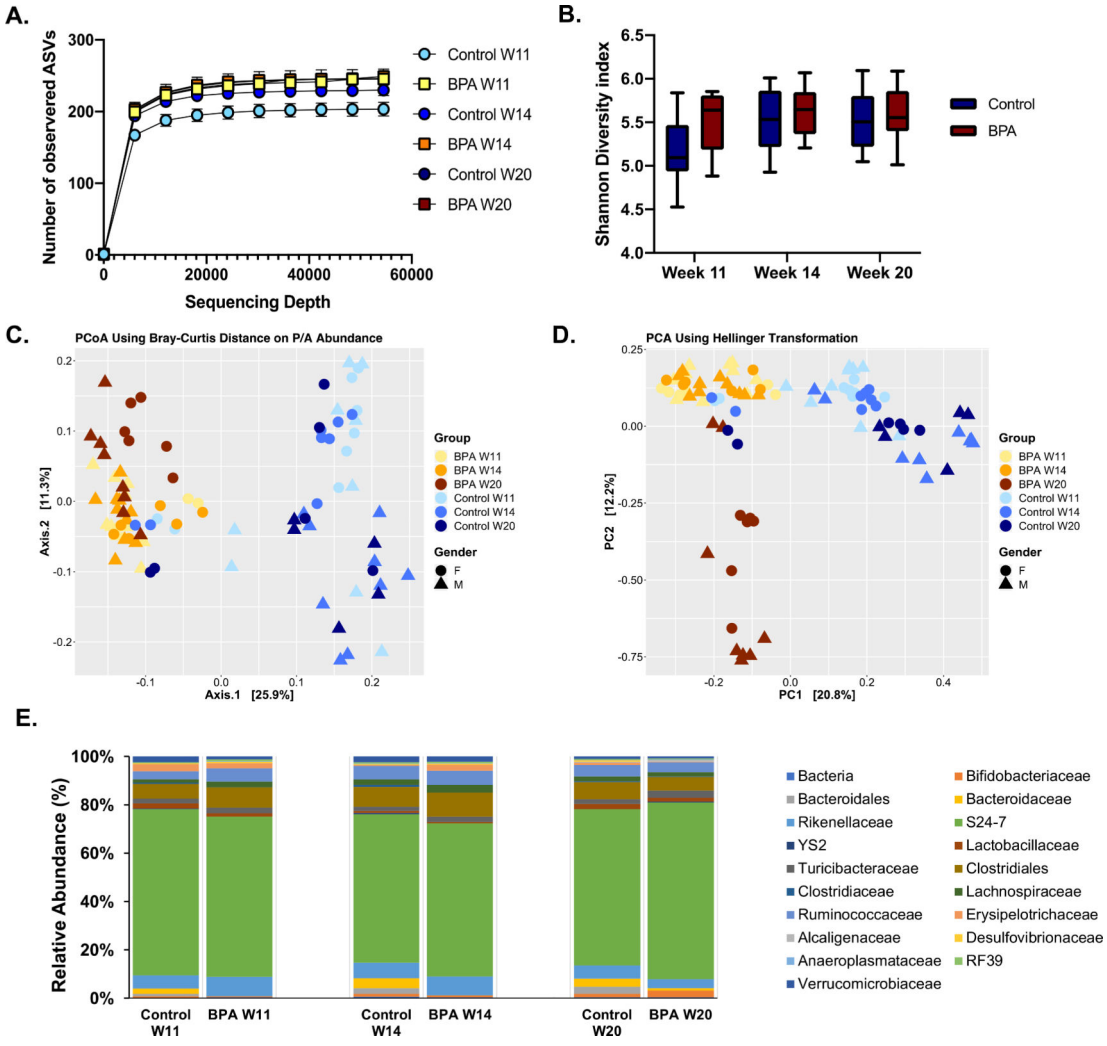


**Fig. 4.**

Gut microbiome diversity in mice offspring exposed to BPA *in utero*. Rarefaction plot using observed amplicon sequence variants (ASVs) comparing fecal profiles of offspring exposed to BPA *in utero* (A). Box-and-whiskers plots of Shannon diversity index of fecal profiles from offspring exposed to BPA *in utero* (B). PCoA using Bray-Curtis distance metrics of offspring fecal profiles exposed to BPA *in utero* (C). PCA using Hellinger-transformed abundances of fecal samples offspring exposed to BPA *in utero* (D). Each dot represents the fecal microbiota of each mouse at week 11 (W11), week 14 (W14), and week 20 (W20). Taxa bar plot of most abundant bacterial families in offspring fecal samples at different time points (W11, W14 and W20) after *in utero* exposure to BPA (E). Sample size n = 6–10 per group/time/sex.

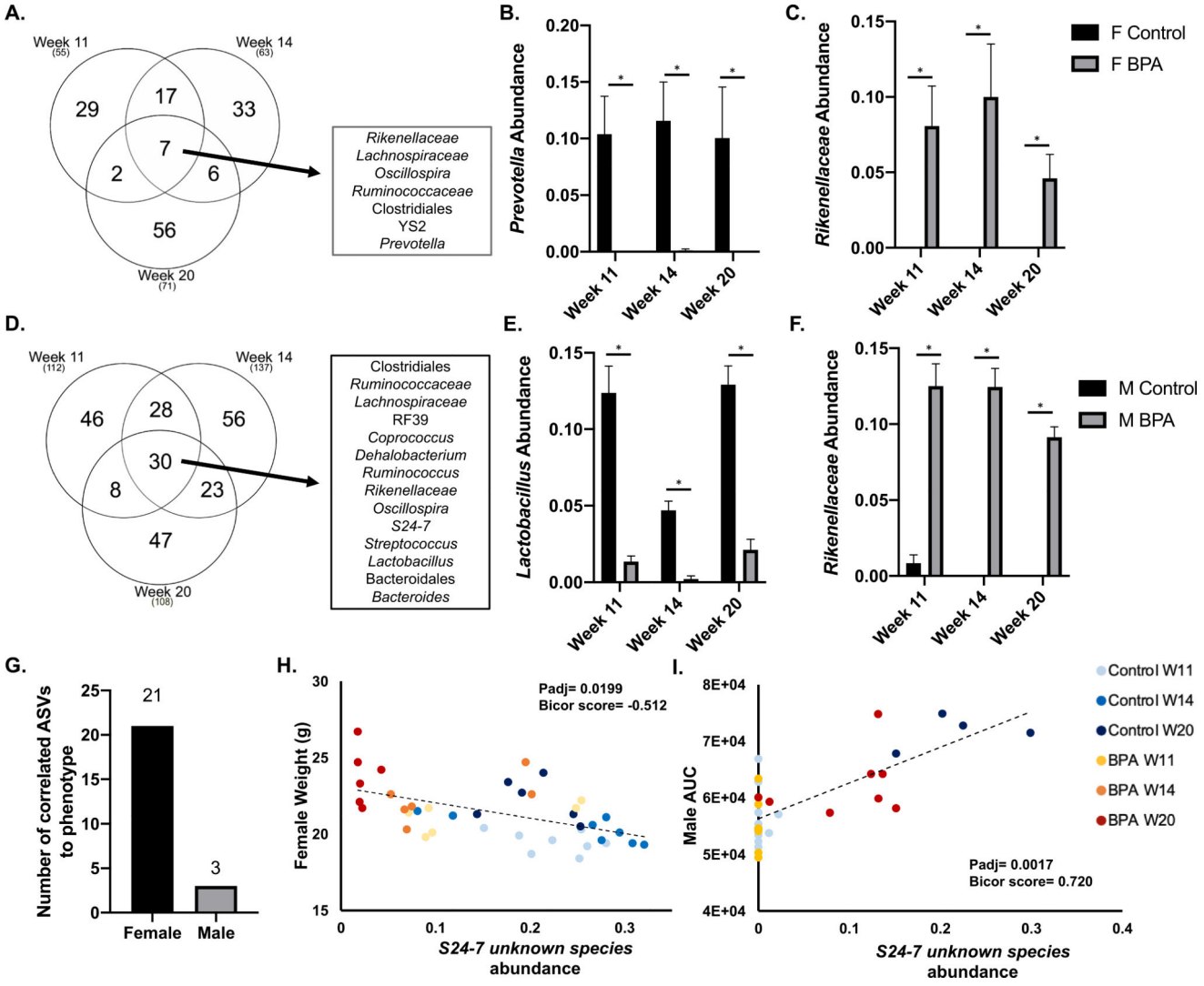


**Fig. 5.**

Taxonomic composition at different time points of offspring exposed to low-dose BPA *in utero.* Venn diagram representing the number of unique and shared differentially abundant amplicon sequence variants (ASVs) at each time point in female fecal samples (A). Bar plots of the abundance of *Prevotella* (B) and *Rikenellaceae unknown species* (C) at all time points in females. Venn diagram representing the number of unique and shared differentially abundant ASVs at each time point in male (D) fecal samples. Bar plots of the abundance of *Lactobacillus* (E) and *Rikenellaceae unknown species* (F) at all time points in males. Bar plot data are presented as mean abundance ± SEM. Bar plot of the number of ASVs significantly correlated to female and male phenotypes (G). Correlation plot between *S24–7 unknown species* abundance and female body weight (H). Correlation plot between *S24–7 unknown species* abundance and male glucose tolerance AUC (I). Bicor score = Biweight midcorrelation (bicor) coefficient, Padj = Benjamini-Hochberg adjusted P-values. Sample size n = 6–10 per group/time/sex.

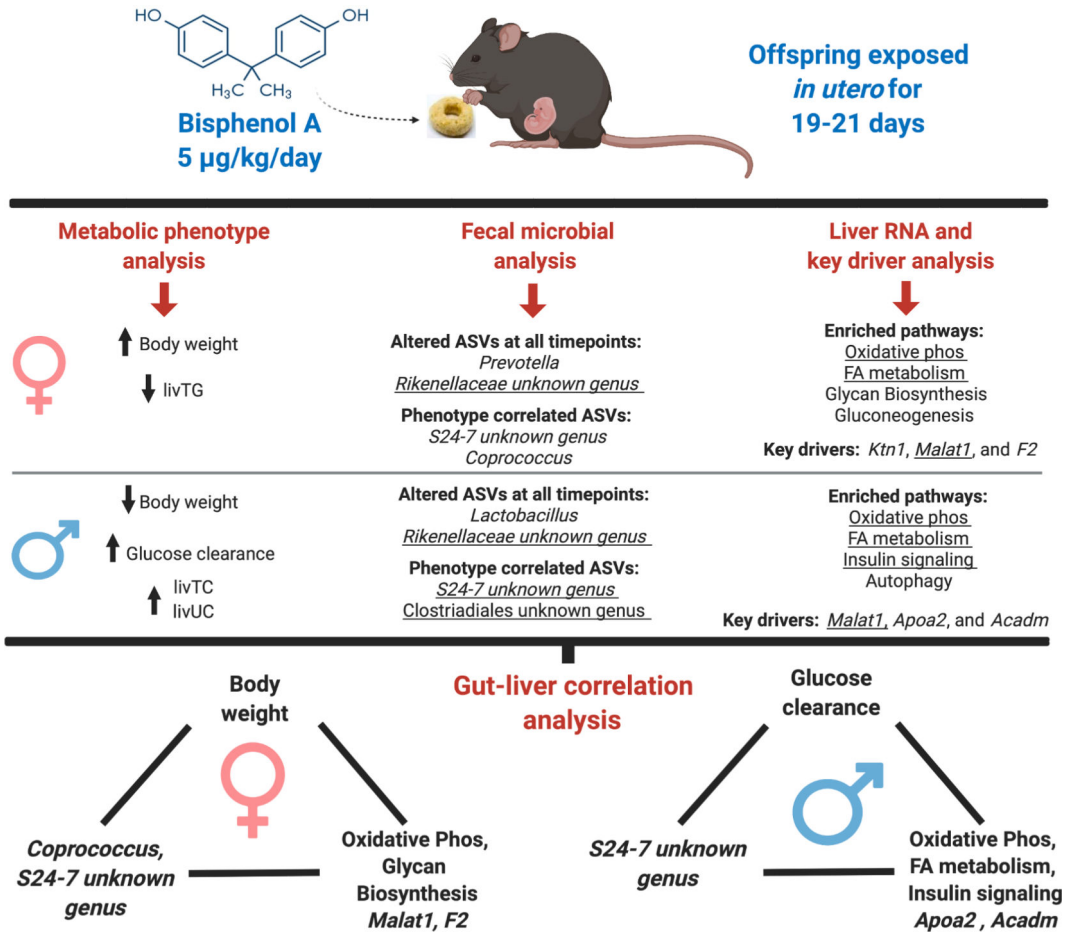


**Fig. 6.**

Summary of the effects of *in utero* BPA exposure on liver metabolic pathways, gut microbiota, and metabolic phenotypes. Underline denotes shared between male and female offspring. Fatty acid metabolism (FA metabolism); Oxidative phosphorylation (Oxidative phos).

**Table 1**

Correlation between BPA altered microbiota and liver DEGs in offspring.

| | Taxa of correlated ASVs | No. of Correlated DEGs BH padj < 0.05 | Enriched KEGG Pathways | Correlated Key Drivers |
|---|---|---|---|---|
| Female | *S24–7* unknown species | 1678 | Oxidative Phosphorylation, Neurodegenerative diseases, RNA metabolism, Citrate cycle, Insulin signaling pathway, PPAR signaling pathway, Glycan biosynthesis | *Ktn1, Golga4, F2, Gcc2, Gls2, Aasdhppt, Qdpr, Plod3, Tlk1, Hmgcl, Hspa1b, Cryl1, Gnmt, Malat1, Apoc3, Dnajb1, Esf1* |
| | Clostridiales unknown species | 1660 | Oxidative Phosphorylation, Neurodegenerative diseases, Lysosome, PPAR signaling pathway, Insulin signaling pathway | *Ktn1, Golga4, F2, Gcc2, Gls2, Aasdhppt, Qdpr, Plod3, Tlk1, Hmgcl, Hspa1b, Cryl1, Gnmt, Apoc3, Dnajb1, Esf1, Dcxr* |
| | *Coprococcus* | 1140 | Oxidative Phosphorylation, Neurodegenerative diseases, Citrate cycle, RNA metabolism, Insulin signaling pathway | *Ktn1, Golga4, F2, Gls2, Qdpr, Plod3, Hspa1b, Cryl1, Malat1, Dnajb1* |
| | YS2 unknown species | 867 | Oxidative Phosphorylation, Neurodegenerative diseases, Citrate cycle, Endocytosis, Amino acid metabolism | *F2, Gls2, Qdpr, Plod3, Tlk1, Cryl1, Atp2a2, Dnajb1* |
| | Clostridiales unknown species | 11 | none | none |
| | *Lachnospiraceae* unknown species | 9 | none | none |
| | *S24–7* unknown species | 1 | none | none |
| Male | Clostridiales unknown species | 1394 | Neurodegenerative disease, Oxidative phosphorylation, Amino acid metabolism, PPAR signaling pathway, Fatty acid metabolism, Drug metabolism, mTOR signaling | *Apoa2, Sepp1, Tlk1, Akr1c12, Erbb2ip, Angptl3, Maob, Hrsp12, Dynlt3, Pebp1, Fabp1, Fbxo31, Acadm, Malat1* |
| | *S24–7* unknown species | 522 | Amino acid metabolism, Propanoate, metabolism, Neurodegenerative disease, Oxidative phosphorylation, Fatty acid metabolism, Insulin signaling pathway, mTOR signaling | *Apoa2, Akr1c12, Angptl3, Maob, Hrsp12, Dynlt3, Acadm* |

Amplicon sequence variants (ASVs); Benjamini-Hochberg adjusted p value (BH padj).